Neural, Parallel, and Scientific Computations 16 (2008) 405-418

AN EFFICIENT NUMERICAL SCHEME FOR SINGULARLY PERTURBED PARABOLIC PROBLEMS WITH INTERIOR LAYER

KAUSHIK MUKHERJEE AND SRINIVASAN NATESAN

Department of Mathematics, Indian Institute of Technology
Guwahati - 781 039, India
Department of Mathematics, Indian Institute of Technology
Guwahati - 781 039, India

ABSTRACT. In this article, a class of singularly perturbed parabolic initial-boundary-value problems possessing strong interior layer due to discontinuous convection coefficient are considered. To solve these problems, we propose a numerical scheme which comprises of classical backward-Euler method for the time discretization and a hybrid finite difference scheme (which is a proper combination of the midpoint upwind scheme in the outer regions and the classical central difference scheme in the interior layer regions) for the spatial discretization. Computationally we show that the proposed numerical scheme is uniformly convergent with respect to the singular perturbation parameter. This is accomplished by constructing a special rectangular mesh involving a piecewise-uniform Shishkin mesh for the spatial variable. Further, we show higher order accuracy of the proposed scheme by comparing it with a classical implicit upwind finite difference scheme.

Key Words. Singularly perturbed parabolic problem, interior layer, numerical scheme, piecewise-uniform Shishkin mesh, uniform convergence.

AMS Subject Classification. 65M06, CR G1.8

1. INTRODUCTION

Consider the following class of singularly perturbed parabolic initial-boundary-value problems posed on the domain denoted by $D = G^- \cup G^+$, $G^- = \Omega^- \times (0,T]$, $G^+ = \Omega^+ \times (0,T]$, $G = \Omega \times (0,T]$, $\Omega^- = (0,\xi)$, $\Omega^+ = (\xi,1)$, $\Omega = (0,1)$:

$$(1.1)\quad \begin{cases} L_\varepsilon u(x,t) \equiv \Big(\varepsilon u_{xx} + a(x)u_x - b(x)u - u_t\Big)(x,t) \;=\; f(x,t), \quad (x,t) \in D \\ u(x,0) = s_0(x), \quad x \in \overline{\Omega} = [0,1], \\ u(0,t) = s_1(t), \quad u(1,t) = s_2(t), \quad t \in (0,T], \end{cases}$$

where $0 < \varepsilon \ll 1$ is a small parameter, the convection coefficient a is sufficiently smooth on $\Omega^- \cup \Omega^+$, the source term f is sufficiently smooth on D and the reaction

Received January 30, 2008

coefficient b is sufficiently smooth on $\overline{\Omega}$ such that

$$\begin{cases} 0 \le \tilde{b} \le b(x) < b^* \quad \text{on } \overline{\Omega}, \\ \big|[a]\big| \le C, \quad \big|[f]\big| \le C, \quad \text{at } x = \xi, \end{cases} \tag{1.2}$$

and the solution $u(x,t)$ satisfies the following interface conditions

$$[u] = 0, \quad [u_x] = 0, \quad \text{at } x = \xi. \tag{1.3}$$

Here $[w]$ denotes the jump in the function w across the point of discontinuity $x = \xi$, *i.e.*, $[w](\xi) = w(\xi+) - w(\xi-)$. In general, due to the presence of discontinuity in the convection coefficient $a(x)$, the solution $u(x,t)$ of the problem (1.1)–(1.3) possesses an interior layer in the neighborhood of the point $x = \xi$. But in reality, the nature of the interior layer depends on the sign of the convection coefficient a either side of the line of discontinuity. Therefore, to emphasize the occurrence of strong interior layer, we consider the following particular case:

$$\begin{cases} -\alpha_1^* < a(x) < -\alpha_1 < 0, & x < \xi, \\ \alpha_2^* > a(x) > \alpha_2 > 0, & x > \xi. \end{cases} \tag{1.4}$$

Note that the coefficients in the differential operator are assumed to be independent of time and we confine here our assumptions to discontinuities in the spatial variable x only. We also assume that the initial and boundary values s_0, s_1 and s_2 are sufficiently smooth on $\overline{G}$ and satisfy the compatibility conditions at the two corners $(0,0), (1,0)$ and at the transition corner point $(\xi, 0)$. These hypotheses guarantee the existence of a unique smooth solution u of the problem (1.1)–(1.4) [4, 9].

Singularly perturbed problems with non-smooth data have been studied many times by several authors, mainly Farrell et al. [5], Linβ [8], Shanthi et al. [10] for stationary case and O'Riordan et al. [4, 9], Shishkin [11, 12, 13] for parabolic problems. These types of problems arise in several branches of engineering and applied mathematics, including convection-dominated flows in fluid mechanics, heat and mass transfer in chemical and nuclear engineering, electromagnetic field etc. Recently, Natesan et al. [7] developed a robust numerical method for time-dependent reaction-diffusion problems exhibiting parabolic boundary layers, which consists of the backward Euler scheme for the time derivative, and a combination of cubic spline scheme and classical finite difference scheme for the spatial derivatives. Also, in [3], they devised two higher-order time accurate numerical schemes for singularly perturbed parabolic initial-boundary-value problems.

In this article, we consider a class of singularly perturbed parabolic convection-diffusion problems whose solutions exhibit strong interior layer caused by the discontinuous convection coefficient. For such type of problems, it is a matter of big challenge to provide ε-uniform numerical methods based on piecewise-uniform Shishkin

meshes. Again, a numerical scheme with a better accuracy is always an attractive feature. Therefore, to accomplish this purpose we propose here an ε-uniform convergent numerical scheme which consists of the backward-Euler scheme for the time discretization and a hybrid scheme (which is a proper combination of a midpoint upwind scheme and the classical central difference scheme) for the spatial discretization. The hybrid scheme was used in [14] for stationary singular perturbation problems (SPPs) with continuous data. Recently, Cen [1] has done the analysis with the same hybrid scheme for stationary SPPs with discontinuous convection coefficient. Here, we devise a hybrid numerical scheme for time-dependent convection-dominated problems with discontinuous convection coefficient.

The rest of the article is organized as follows: In Section 2, we describe the numerical scheme by introducing a rectangular mesh for discretization of the domain. Section 3 provides the classical implicit upwind finite difference scheme [9] for comparison purpose and also present the numerical results for both the schemes. The paper ends with a brief conclusion.

2. NUMERICAL APPROXIMATION

In this section, we construct a suitable mesh for the discretization of the domain to obtain an ε-uniform convergent difference scheme and also explicitly describe the difference scheme used to discretize the problem (1.1)–(1.4).

2.1. **Discretization of the Domain.** Consider the domain $\overline{G} \equiv \overline{\Omega} \times [0,T] = [0,1] \times [0,T]$ and let $N \geq 4$ be a positive even integer. Here, we will construct a rectangular mesh $\overline{G}_{\varepsilon}^{N,M} = \overline{\Omega}_{x}^{N,\varepsilon} \times \mathbb{S}_{t}^{M}$, which is a combination of the piecewise-uniform Shishkin mesh condensed around the interior layer for the spatial variable and a uniform mesh for the temporal variable. Firstly, on the spatial domain $\overline{\Omega}$, we define the piecewise-uniform Shishkin mesh by subdividing $\overline{\Omega}$ into four subintervals as $\overline{\Omega} = [0, \xi - \sigma_1] \cup [\xi - \sigma_1, \xi] \cup [\xi, \xi + \sigma_2] \cup [\xi + \sigma_2, 1]$ for some σ_1, σ_2 that satisfy $0 < \sigma_1 \leq \xi/2$, $0 < \sigma_2 \leq (1-\xi)/2$. On each subinterval a uniform mesh with $N/4$ mesh-intervals is placed and

$$\Omega_{x}^{N,\varepsilon} = \{x_i : 1 \leq i \leq N/2 - 1\} \bigcup \{x_i : N/2 + 1 \leq i \leq N - 1\}$$

denotes the set of interior points of the mesh. Clearly $x_{N/2} = \xi$ and $\overline{\Omega}_{x}^{N,\varepsilon} = \{x_i\}_{0}^{N}$. Note that this is a uniform mesh when $\sigma_1 = \xi/2,\ \sigma_2 = (1-\xi)/2$. It is fitted to the problem (1.1)–(1.4) by choosing σ_1 and σ_2 to be the following functions of N and ε

$$\sigma_1 = \min\left\{\frac{\xi}{2}, \frac{2\varepsilon}{\alpha}\ln N\right\}, \quad \sigma_2 = \min\left\{\frac{1-\xi}{2}, \frac{2\varepsilon}{\alpha}\ln N\right\},$$

where $\alpha = \min\{\alpha_1, \alpha_2\}$. On the time domain $[0, T]$, we introduce the equidistant meshes in the temporal variable such that

$$\mathbb{S}_t^M = \{t_n = n\,\Delta t,\, n = 0, \ldots, M,\ t_0 = 0, t_M = T,\ \Delta t = T/M\},$$

where M denotes the number of mesh elements in the t-direction. Let us denote the step sizes in space by

$$h_i = x_i - x_{i-1},\ i = 1, \ldots, N, \quad \widehat{h}_i = h_i + h_{i+1},\ i = 1, \ldots, N-1.$$

Further, denote the mesh width h_i in the spatial direction as follows:

$$h_i = \begin{cases} H_{(l)} = 4(\xi - \sigma_1)/N & i = 1, \ldots, N/4, \\ h_{(l)} = 4\sigma_1/N & i = N/4+1, \ldots, N/2-1, \\ h_{(r)} = 4\sigma_2/N & i = N/2+1, \ldots, 3N/4, \\ H_{(r)} = 4(1-\xi-\sigma_2)/N & i = 3N/4+1, \ldots, N. \end{cases}$$

2.2. **The Backward-Euler Hybrid Finite Difference Scheme.** Here, for the discretization of the problem (1.1)–(1.4) in the spatial variable, we propose a hybrid scheme. The hybrid scheme consists of the midpoint upwind scheme in the outer regions $[0, \xi - \sigma_1], [\xi + \sigma_2, 1]$ and the classical central difference scheme in the interior layer regions $(\xi - \sigma_1, \xi), (\xi, \xi + \sigma_2)$. While for the temporal discretization, we employ the standard backward-Euler scheme. Before describing the scheme, for a given mesh function $v(x_i, t_n) = v_i^n$, define the forward, backward and central difference operators D_x^+, D_x^- and D_x^0 in space and the backward difference operator D_t^- in time by

$$\text{(2.1)} \qquad \begin{cases} D_x^+ v_i^n = \dfrac{v_{i+1}^n - v_i^n}{h_{i+1}},\ D_x^- v_i^n = \dfrac{v_i^n - v_{i-1}^n}{h_i},\ D_x^0 v_i^n = \dfrac{v_{i+1}^n - v_{i-1}^n}{\widehat{h}_i} \\ \text{and} \quad D_t^- v_i^n = \dfrac{v_i^n - v_i^{n-1}}{\Delta t}, \end{cases}$$

respectively, and also define $v_{i\mp1/2}^n = \big(v_{i\mp1}^n + v_i^n\big)/2$. Note that when $v(x_i) = v_i$, we similarly define $v_{i\mp1/2} = \big(v_{i\mp1} + v_i\big)/2$. Then, the proposed numerical scheme is of the following form:

$$\text{(2.2)} \qquad \begin{cases} L_{mu}^{N,M,(-)} U_i^{n+1} = f_{i-1/2}^{n+1} & \text{for } i = 1, \ldots, N/4, \\ L_{cen}^{N,M} U_i^{n+1} = f_i^{n+1} & \text{for } i = N/4+1, \ldots, N/2-1, \\ & \qquad N/2+1, \ldots, 3N/4-1, \\ L_{mu}^{N,M,(+)} U_i^{n+1} = f_{i+1/2}^{n+1} & \text{for } i = 3N/4, \ldots, N-1, \\ D_x^F\, U_i^{n+1} - D_x^B\, U_i^{n+1} = 0 & \text{for } i = N/2, \end{cases}$$

where

$$
(2.3)\quad \begin{cases} L_{mu}^{N,M,(-)}U_i^{n+1} &= \varepsilon D_x^+ D_x^- U_i^{n+1} + a_{i-1/2} D_x^- U_i^{n+1} - b_{i-1/2} U_{i-1/2}^{n+1} \\ & \quad -D_t^- U_{i-1/2}^{n+1}, \\ L_{cen}^{N,M} U_i^{n+1} &= \varepsilon D_x^+ D_x^- U_i^{n+1} + a_i D_x^0 U_i^{n+1} - b_i U_i^{n+1} - D_t^- U_i^{n+1}, \\ L_{mu}^{N,M,(+)}U_i^{n+1} &= \varepsilon D_x^+ D_x^- U_i^{n+1} + a_{i+1/2} D_x^+ U_i^{n+1} - b_{i+1/2} U_{i+1/2}^{n+1} \\ & \quad -D_t^- U_{i+1/2}^{n+1}, \end{cases}
$$

and

$$
(2.4)\quad D_x^F U_i^n = (-U_{i+2}^n + 4U_{i+1}^n - 3U_i^n)/2h_{(r)}, \quad D_x^B U_i^n = (U_{i-2}^n - 4U_{i-1}^n + 3U_i^n)/2h_{(l)}.
$$

After rearranging the terms in (2.2), we obtain the following complete form of the difference scheme on the mesh $\overline{G}_\varepsilon^{N,M}$:

$$
(2.5)\quad \begin{cases} \begin{cases} L_{hyb}^{N,M} U_i^{n+1} \equiv \left[r_i^- U_{i-1}^{n+1} + r_i^0 U_i^{n+1} + r_i^+ U_{i+1}^{n+1}\right] \\ \qquad\qquad + \left[p_i^- U_{i-1}^n + p_i^0 U_i^n + p_i^+ U_{i+1}^n\right] \\ \qquad\qquad = \left[m_i^- f_{i-1}^{n+1} + m_i^0 f_i^{n+1} + m_i^+ f_{i+1}^{n+1}\right], \\ \qquad\qquad\quad \text{for } i = 1, \ldots, N/2-1, N/2+1, \ldots, N-1, \\ q_i^{-,2} U_{i-2}^{n+1} + q_i^{-,1} U_{i-1}^{n+1} + q_i^0 U_i^{n+1} + q_i^{+,1} U_{i+1}^{n+1} + q_i^{+,2} U_{i+2}^{n+1} = 0, \\ \qquad\qquad\quad \text{for } i = N/2, \end{cases} \\ U_i^0 = s_0(x_i), \quad \text{for } i = 0, \ldots, N, \\ U_0^{n+1} = s_1(t_{n+1}), \quad U_N^{n+1} = s_2(t_{n+1}), \\ \text{for } n = 0, \ldots, M-1, \end{cases}
$$

where, for $i = 1, \ldots, N/4$, the coefficients are given by

$$
(2.6)\quad \begin{cases} r_i^- &= \left(\dfrac{2\varepsilon}{\widehat{h}_i h_i} - \dfrac{a_{i-1/2}}{h_i} - \dfrac{b_{i-1/2}}{2}\right) - \dfrac{1}{2\Delta t}, \\ r_i^0 &= \left(-\dfrac{2\varepsilon}{h_i h_{i+1}} + \dfrac{a_{i-1/2}}{h_i} - \dfrac{b_{i-1/2}}{2}\right) - \dfrac{1}{2\Delta t}, \\ r_i^+ &= \dfrac{2\varepsilon}{\widehat{h}_i h_{i+1}}, \\ p_i^- = \dfrac{1}{2\Delta t}, \quad p_i^0 = \dfrac{1}{2\Delta t}, \quad p_i^+ = 0, \\ m_i^- = \dfrac{1}{2}, \quad m_i^0 = \dfrac{1}{2}, \quad m_i^+ = 0, \end{cases}
$$

and for $i = N/4+1, \ldots, N/2-1, N/2+1, \ldots, 3N/4-1$,

$$\text{(2.7)} \qquad \begin{cases} r_i^- = \left(\dfrac{2\varepsilon}{\widehat{h}_i h_i} - \dfrac{a_i}{\widehat{h}_i}\right), \\ r_i^0 = \left(-\dfrac{2\varepsilon}{h_i h_{i+1}} - b_i\right) - \dfrac{1}{\Delta t}, \\ r_i^+ = \left(\dfrac{2\varepsilon}{\widehat{h}_i h_{i+1}} + \dfrac{a_i}{\widehat{h}_i}\right), \\ p_i^- = 0, \quad p_i^0 = \dfrac{1}{\Delta t}, \quad p_i^+ = 0, \\ m_i^- = 0, \quad m_i^0 = 1, \quad m_i^+ = 0, \end{cases}$$

and for $i = 3N/4, \ldots, N-1$,

$$\text{(2.8)} \qquad \begin{cases} r_i^- = \dfrac{2\varepsilon}{\widehat{h}_i h_i}, \\ r_i^0 = \left(-\dfrac{2\varepsilon}{h_i h_{i+1}} - \dfrac{a_{i+1/2}}{h_{i+1}} - \dfrac{b_{i+1/2}}{2}\right) - \dfrac{1}{2\Delta t}, \\ r_i^+ = \left(\dfrac{2\varepsilon}{\widehat{h}_i h_{i+1}} + \dfrac{a_{i+1/2}}{h_i} - \dfrac{b_{i+1/2}}{2}\right) - \dfrac{1}{2\Delta t}, \\ p_i^- = 0, \quad p_i^0 = \dfrac{1}{2\Delta t}, \quad p_i^+ = \dfrac{1}{2\Delta t}, \\ m_i^- = 0, \quad m_i^0 = \dfrac{1}{2}, \quad m_i^+ = \dfrac{1}{2}, \end{cases}$$

and lastly, for $i = N/2$,

(2.9)

$$q_i^{-,2} = -h_{(r)}, \quad q_i^{-,1} = 4h_{(r)}, \quad q_i^0 = -3\big(h_{(r)} + h_{(l)}\big), \quad q_i^{+,1} = 4h_{(l)}, \quad q_i^{+,2} = -h_{(l)}.$$

The tridiagonal system of equations will be solved by a suitable solver to obtain the numerical solution at the $(n+1)$th level. The stability and error analysis of the proposed numerical scheme will be carried out in our working paper [6].

3. NUMERICAL RESULTS

In this section, we shall present the numerical results obtained by the newly proposed scheme (2.5) for two test problems and compare the numerical performance with a standard first-order implicit upwind scheme on the piecewise-uniform rectangular mesh $\overline{G}_\varepsilon^{N,M}$. In all the cases, we execute the numerical experiments by choosing $N = 16\times 2^i$ and correspondingly, $\Delta t = 0.1/2^{i+1}$, $i = 0, 1, \ldots, 6$ such that $\Delta t = 0.8/N$. Note that though we have done the computations for $\varepsilon = 10^{-1}, \ldots, 10^{-10}$, to make explanation more precise we have displayed the numerical results only for $\varepsilon = 10^{-1}, 10^{-5}$ and 10^{-10}.

3.1. **The Classical Implicit Upwind Scheme.** To show the higher-order accuracy of the proposed method, we compare the numerical results with the classical first-order implicit upwind scheme proposed by O'Riordan et al. [9] for the problem (1.1)–(1.4). In this scheme, they use the backward-Euler method for time and the classical upwind finite difference scheme for spatial discretization on the piecewise-uniform rectangular mesh $\overline{G}_\varepsilon^{N,M}$:

$$
\left\{
\begin{array}{l}
\left\{
\begin{array}{l}
L_{up}^{N,M} U_i^{n+1} \equiv \varepsilon D_x^+ D_x^- U_i^{n+1} + a_i D_x^* U_i^{n+1} - b_i U_i^{n+1} - D_t^- U_i^{n+1} \\
\qquad\qquad = f_i^{n+1}, \quad \text{for } i = 1, \ldots, N/2-1, N/2+1, \ldots, N-1, \\
D_x^+ U_i^{n+1} - D_x^- U_i^{n+1} = 0, \quad \text{for } i = N/2,
\end{array}
\right. \\
U_i^0 = s_0(x_i), \quad \text{for } i = 0, \ldots, N, \\
U_0^{n+1} = s_1(t_{n+1}), \quad U_N^{n+1} = s_2(t_{n+1}), \\
\text{for } n = 0, \ldots, M-1,
\end{array}
\right. \tag{3.1}
$$

where

$$
D_x^* U_i^n = \begin{cases} D_x^- U_i^n, & i < N/2, \\ D_x^+ U_i^n, & i > N/2, \end{cases}
$$

the finite difference operators D_x^-, D_x^+, D_t^- are defined in (2.1).

3.2. **Numerical Examples.** To show the efficiency of the proposed numerical scheme (2.5), we implement it to two test problems which have no exact solutions. Therefore, to obtain the accuracy of the numerical solution and also to demonstrate the ε-uniform convergence of the proposed scheme, we use the double mesh principle as in [2] which is described below.

Let $U^{N,\Delta t}(x_i, t_n)$ be the numerical solution on the mesh $\overline{G}_\varepsilon^{N,M}$ with N mesh intervals in the spatial direction and M mesh intervals in the t-direction such that $\Delta t = T/M$ is the uniform time step. Also, let $\widetilde{U}^{2N,\Delta t/2}(x_i, t_n)$ be the piecewise linear interpolant obtained from the numerical solution $U^{2N,\Delta t/2}(x_i, t_n)$ defined on the coarse mesh $\overline{G}_\varepsilon^{N,M}$. Note that no special interpolation is required for the time variable because $\mathbb{S}_t^M = \mathbb{S}_t^{2M} \cap \mathbb{S}_t^M$. Then for each ε, we can calculate the maximum point-wise error by

$$
E_\varepsilon^{N,\Delta t} = \max_{(x_i,t_n) \in \overline{G}_\varepsilon^{N,M}} \left| U^{N,\Delta t}(x_i, t_n) - \widetilde{U}^{2N,\Delta t/2}(x_i, t_n) \right|,
$$

and the corresponding order of convergence by

$$
P_\varepsilon^{N,\Delta t} = \log_2 \left(\frac{E_\varepsilon^{N,\Delta t}}{E_\varepsilon^{2N,\Delta t/2}} \right).
$$

Now, for each N and Δt, define $E^{N,\Delta t} = \max_{\varepsilon} E_{\varepsilon}^{N,\Delta t}$ as the ε-uniform maximum point-wise error and the corresponding local ε-uniform order of convergence is defined by

$$P^{N,\Delta t} = \log_2\left(\frac{E^{N,\Delta t}}{E^{2N,\Delta t/2}}\right).$$

Example 3.1. Consider the parabolic initial-boundary value problem studied by Dunne et al. [4]:

$$\begin{cases} \varepsilon u_{xx} + a(x)u_x - u_t = f(x,t), \quad (x,t) \in (0,1)\times(0,1] \\ u(x,0) = 0, \quad 0 \le x \le 1, \\ u(0,t) = t^2, \quad u(1,t) = 0, \quad 0 < t \le 1, \end{cases} \tag{3.2}$$

where the source term

$$f(x,t) = \begin{cases} 2xt, & 0 \le x \le 0.5, \\ 2(1-x)t, & 0.5 < x \le 1, \end{cases}$$

and the convective coefficient

$$a(x) = \begin{cases} -1, & 0 \le x \le 0.5, \\ 1, & 0.5 < x \le 1. \end{cases}$$

The computed maximum point-wise errors $E_{\varepsilon}^{N,\Delta t}$, the corresponding order of convergence $P_{\varepsilon}^{N,\Delta t}$ and the computed ε-uniform errors $E^{N,\Delta t}$, the corresponding ε-uniform order of convergence $P^{N,\Delta t}$ for Example 3.1 are presented in Table 1 for various values of ε and N.

Example 3.2. Consider the following parabolic initial-boundary value problem with variable convection coefficient:

$$\begin{cases} \varepsilon u_{xx} + a(x)u_x - u_t = f(x,t), \quad (x,t) \in (0,1)\times(0,1] \\ u(x,0) = 0, \quad 0 \le x \le 1, \\ u(0,t) = 0, \quad u(1,t) = 0, \quad 0 < t \le 1, \end{cases} \tag{3.3}$$

where the source term

$$f(x,t) = \begin{cases} 2xt, & 0 \le x \le 0.5, \\ 2(1-x)t, & 0.5 < x \le 1, \end{cases}$$

and the convective coefficient

$$a(x) = \begin{cases} -2(1+x), & 0 \le x \le 0.5, \\ 3-2x, & 0.5 < x \le 1. \end{cases}$$

As like in the previous example, the corresponding numerical results for Example 3.2 have been depicted in Table 2.

From Tables 1 and 2 we see that for $N \geq 16$, the ε-uniform error $E^{N,\Delta t}$ decreases monotonically as N increases. This ensures that the proposed numerical scheme (2.5) is of ε -uniform convergent. As a complement of this observation, we have plotted the maximum point-wise errors for Examples 3.1 and 3.2 in Figure 1. We have also included some surface plots of the numerical solutions of Examples 3.1 and 3.2 in Figure 2 to visualize clearly the interior layers.

Next, we have done the numerical comparison between the proposed numerical scheme (2.5) and the implicit upwind finite difference scheme (3.1) through Tables 3 and 4 for Examples 3.1 and 3.2 respectively. These comparisons strengthen the fact that the proposed scheme (2.5) performs numerically better than the first-order implicit upwind finite difference scheme in all cases. Mainly, it is observed that though the backward-Euler method used for the time discretization in both the schemes is of first order accurate in time, the use of the hybrid scheme for the spatial discretization increases the numerical order of convergence as well as the ε-uniform order of convergence of the proposed numerical scheme (2.5). To make this analysis more significant, we have highlighted the comparison of the errors between both the schemes for Examples 3.1 and 3.2 respectively in Figures 3 and 4.

4. CONCLUSIONS

In this article, we have devised a numerical scheme for a class of singularly perturbed parabolic initial-boundary value problems with discontinuous convection coefficient. The proposed numerical scheme comprises of the backward-Euler scheme for the time discretization and a hybrid finite difference scheme for the spatial discretization. For the construction of the numerical scheme, we have used a piecewise-uniform Shishkin mesh fitted to the interior layer for discretization of the spatial domain and a uniform mesh for the temporal domain. It has been experimented computationally through some examples that the proposed numerical scheme is of ε-uniform convergent. Moreover, we have also shown that the proposed numerical scheme responds well with a better numerical accuracy compared to the classical implicit upwind finite difference scheme. Therefore, looking towards the better numerical performance of the proposed scheme, it can be naturally concluded that one can take the above computational analysis as a motivation for further theoretical analysis of the proposed numerical scheme.

REFERENCES

[1] Z. Cen, A hybrid difference scheme for a singularly perturbed convection-diffusion problem with discontinuous convection coefficient, *Appl. Math. Comput.*, **169**:689–699, 2005.

[2] C. Clavero, J.C. Jorge, and F. Lisbona, A uniformly convergent scheme on a nonuniform mesh for convection-diffusion parabolic problems, *J. Comput. Appl. Math.*, **154**:415–429, 2003.

[3] R. Deb and S. Natesan, Higher-order time accurate numerical methods for singularly perturbed parabolic partial differential equations. *Int. J. Comput. Math.*, 2008 (In Press).

[4] R.K. Dunne and E. O'Riordan, Interior layers arising in linear singularly perturbed differential equations with discontinuous coefficients, Technical report, DCU School of Mathematics, 2006.

[5] P.A. Farrell, A.F. Hegarty, J.J.H. Miller, E. O'Riordan, and G.I. Shishkin, Global maximum norm parameter-uniform numerical method for a singularly perturbed convection-diffusion problem with discontinuous convection coefficient, *Mathematics and Computer Modelling*, **40**:1375–1392, 2004.

[6] K. Mukherjee and S. Natesan, ε-uniform error estimates for singularly perturbed parabolic problems with interior layer, Working paper, 2008.

[7] S. Natesan, and R. Deb, A robust numerical scheme for singularly perturbed parabolic reaction-diffusion problems. *Neural, Parallel, and Scientific Computations*, **xx**: xx–xx, 2008. (To Appear)

[8] T. Linβ, Finite difference schemes for convection-diffusion problems with a concentrated source and discontinuous convective field, *Comput. Methods. Appl. Math.*, **2**:41–49, 2002.

[9] E. O'Riordan and G.I. Shishkin, Singularly perturbed parabolic problems with non-smooth data, *J. Comput. Appl. Math.*, **166**:233–245, 2004.

[10] V. Shanthi, N. Ramanujam, and S. Natesan, Fitted mesh method for singularly perturbed reaction convection-diffusion problems with boundary and interior layers, *J. Appl. Math. & Computing*, **22**(1-2):49–65, 2006.

[11] G. I. Shishkin, A difference scheme for a singularly perturbed equation of parabolic type with discontinuous initial condition, *Soviet Math. Dokl.*, **37**(3):729–796, 1988.

[12] G. I. Shishkin, A difference scheme for a singularly perturbed parabolic equation with discontinuous coefficients and concentrated factors, *U.S.S.R. Comput. Maths. Math. Phys.*, **29**(5):9–15, 1989.

[13] G. I. Shishkin, Approximation of singularly perturbed parabolic reaction-diffusion equations with nonsmooth data, *Comput. Methods. Appl. Math.*, **1**(3):298–315, 2001.

[14] M. Stynes and H.G. Roos, The midpoint upwind scheme, *Appl. Numer. Math.*, **23**:361–374, 1997.

TABLE 1. Maximum point-wise errors and order of convergence corresponding to the numerical scheme (2.5) for Example 3.1.

ε	Number of mesh intervals N						
	16	32	64	128	256	512	1024
$1e-1$	1.1846e-2	4.6571e-3	1.9099e-3	8.8214e-4	4.2631e-4	2.0976e-4	1.0406e-4
	1.3469	1.2859	1.1144	1.0491	1.0232	1.0113	
$1e-5$	2.3049e-2	9.9736e-3	4.1094e-3	1.7641e-3	8.2587e-4	3.9692e-4	1.9593e-4
	1.2085	1.2792	1.2200	1.0949	1.0571	1.0185	
$1e-10$	2.3051e-2	9.9737e-3	4.1095e-3	1.7641e-3	8.2580e-4	3.9691e-4	1.9601e-4
	1.2086	1.2792	1.2200	1.0951	1.0570	1.0179	
$E^{N,\Delta t}$	**2.3051e-2**	**9.9737e-3**	**4.1095e-3**	**1.7886e-3**	**8.2589e-4**	**3.9694e-4**	**1.9601e-4**
$P^{N,\Delta t}$	**1.2086**	**1.2792**	**1.2002**	**1.1148**	**1.0570**	**1.0179**	

TABLE 2. Maximum point-wise errors and order of convergence corresponding to the numerical scheme (2.5) for Example 3.2.

ε	Number of mesh intervals N						
	16	32	64	128	256	512	1024
$1e-1$	2.1864e-3	7.6102e-4	2.5343e-4	8.5841e-5	3.5560e-5	1.7866e-5	8.9537e-6
	1.5226	1.5863	1.5618	1.2714	0.9930	0.9966	
$1e-5$	9.0257e-3	4.3260e-3	1.9090e-3	6.5234e-4	2.6376e-4	1.0243e-4	3.7893e-5
	1.0610	1.1802	1.5491	1.3064	1.3646	1.4346	
$1e-10$	9.0270e-3	4.3263e-3	1.9091e-3	6.5238e-4	2.6399e-4	1.0256e-4	3.6051e-5
	1.0611	1.1803	1.5491	1.3052	1.3641	1.5083	
$E^{N,\Delta t}$	**9.0270e-3**	**4.3263e-3**	**1.9091e-3**	**6.5238e-4**	**2.6399e-4**	**1.0256e-4**	**3.8059e-5**
$P^{N,\Delta t}$	**1.0611**	**1.1803**	**1.5491**	**1.3052**	**1.3641**	**1.4301**	

TABLE 3. Order of convergence corresponding to the numerical scheme (3.1) for Example 3.1.

ε	Number of mesh intervals N					
	16	32	64	128	256	512
$1e-1$	0.9764	0.9883	0.9941	0.9970	0.9985	0.9992
$1e-5$	0.7514	0.9401	1.0032	1.0078	1.0051	0.8604
$1e-10$	0.7512	0.9400	1.0031	1.0077	1.0050	0.8590
$P^{N,\Delta t}$	**0.9764**	**0.9883**	**0.9941**	**0.9970**	**0.8131**	**0.7808**

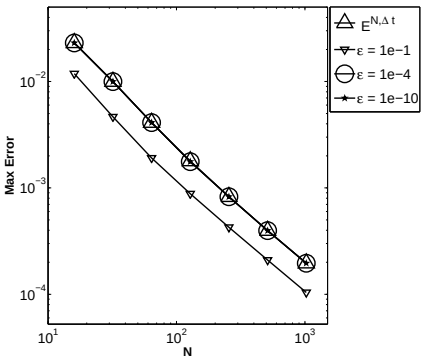

(a) Example 3.1.

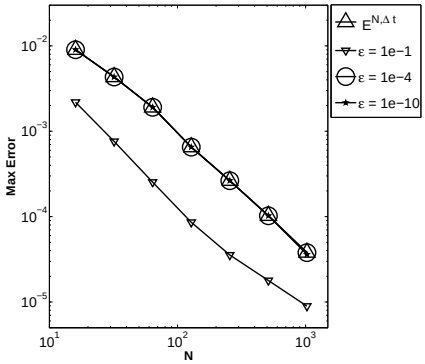

(b) Example 3.2.

FIGURE 1. Loglog plot of the maximum point-wise error obtained by the numerical scheme (2.5).

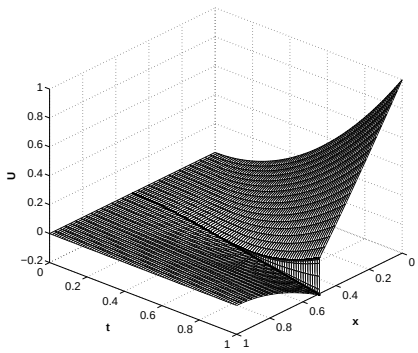

(a) Example 3.1.

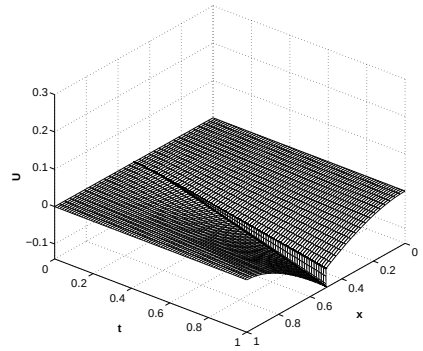

(b) Example 3.2.

FIGURE 2. Numerical solution for $\varepsilon = 1e-4,\ N = 64$ obtained by the numerical scheme (2.5).

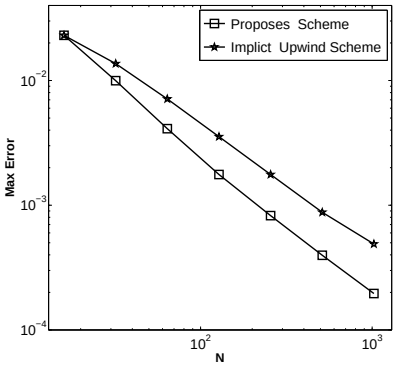

(a) $\varepsilon = 1e-4$.

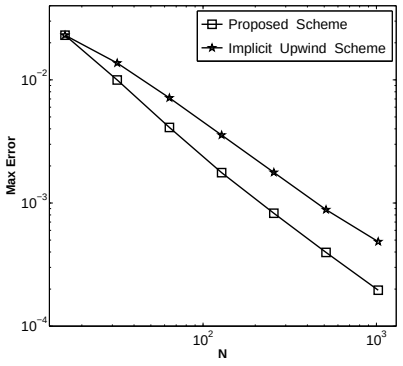

(b) $\varepsilon = 1e-8$.

FIGURE 3. Loglog plot for comparison of the error of Example 3.1.

TABLE 4. Order of convergence corresponding to the numerical scheme (3.1) for Example 3.2.

ε	Number of mesh intervals N					
	16	32	64	128	256	512
$1e-1$	1.1223	1.0222	1.0541	1.0310	1.0184	1.0101
$1e-5$	0.7011	0.6349	0.6258	0.6694	0.6977	0.7451
$1e-10$	0.7010	0.6349	0.6257	0.6693	0.6980	0.7408
$P^{N,\Delta t}$	**0.7010**	**0.6349**	**0.6257**	**0.6693**	**0.6979**	**0.7409**

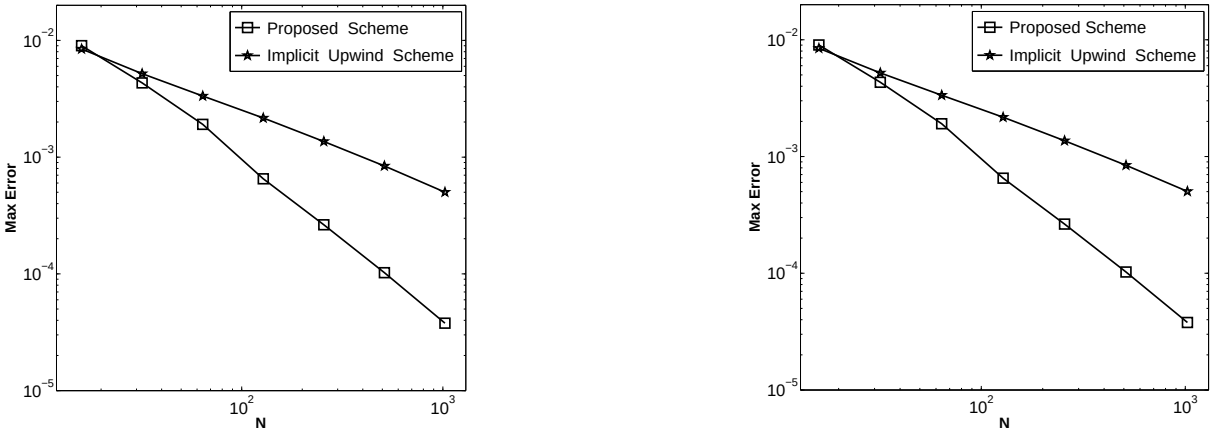

(a) $\varepsilon = 1e-4$. (b) $\varepsilon = 1e-8$.

FIGURE 4. Loglog plot for comparison of the error of Example 3.2.